

Cyclotron effective masses in layered metals

Jaime Merino* and Ross H. McKenzie**

School of Physics, University of New South Wales, Sydney 2052, Australia

(February 1, 2008)

Many layered metals such as quasi-two-dimensional organic molecular crystals show properties consistent with a Fermi liquid description at low temperatures. The effective masses extracted from the temperature dependence of the magnetic oscillations observed in these materials are in the range, $m_c^*/m_e \sim 1 - 7$, suggesting that these systems are strongly correlated. However, the ratio m_c^*/m_e contains both the renormalization due to the electron-electron interaction and the periodic potential of the lattice. We show that for *any* quasi-two-dimensional band structure, the cyclotron mass is proportional to the density of states at the Fermi energy. Due to Luttinger's theorem, this result is also valid in the presence of interactions. We then evaluate m_c for several model band structures for the β , κ , and θ families of $(\text{BEDT-TTF})_2\text{X}$, where BEDT-TTF is bis-(ethylenedithia-tetrathiafulvalene) and X is an anion. We find that for κ -(BEDT-TTF)₂X, the cyclotron mass of the β -orbit, $m_c^{*\beta}$, is close to $2 m_c^{*\alpha}$, where $m_c^{*\alpha}$ is the effective mass of the α - orbit. This result is fairly insensitive to the band structure details. For a wide range of materials we compare values of the cyclotron mass deduced from band structure calculations to values deduced from measurements of magnetic oscillations and the specific heat coefficient γ .

PACS numbers: 71.27.+a, 71.10.Fd

A. Introduction

Quasi-two-dimensional metals such as the organic molecular crystals based on the BEDT-TTF molecule [where BEDT-TTF is bis-(ethylenedithia-tetrathiafulvalene)] and the layered perovskites Sr_2RuO_4 , show properties which are consistent with a Fermi liquid description at low temperatures.¹ Although transport properties of these materials show unconventional behaviour with temperature at high temperatures, at low temperatures (below about 20 K in the organics) the resistivity is quadratic with temperature, the thermopower is linear in temperature and a Drude peak is present in the optical conductivity.² Furthermore, magnetic oscillations such as the de Haas - van Alphen effect is observed^{3,4} suggesting the presence of a well defined Fermi surface and quasiparticle excitations described by Fermi liquid theory. In order to understand the role of electron-electron interactions in these materials it is then necessary to quantify the strength of electron correlations and test how robust the Fermi liquid description is.

Cyclotron effective masses for the quasiparticles can be obtained from fitting the observed temperature dependence of the amplitude of magnetic oscillations to the Lifshitz-Kosevich form. The amplitude at a temperature T is proportional to

$$R_T = \frac{X}{\sinh X} \quad X = \frac{2\pi^2 k_B T}{\hbar \omega_c^*} \quad (1)$$

where $\omega_c^* = eB/m_c^*$ is the cyclotron frequency and m_c^* is the cyclotron effective mass, including many-body effects.

Typical values obtained for the cyclotron mass in these materials are in the range, $m_c^*/m_e \sim 1 - 7$, (where m_e is the free electron mass) suggesting the possibility that many-body effects may cause a significant enhancement of the effective mass. However, knowing m_c^*/m_e by itself is not sufficient to determine the size of many-body effects due to electron-electron and electron-phonon interactions. First, it is necessary to compute the cyclotron band mass, m_c , which takes into account the fact that electrons are not free but are moving in the presence of the periodic potential associated with the crystal lattice. Then, the ratio m_c^*/m_c can be used to estimate the importance of many-body effects. As we will see, estimates of m_c deduced from band structure calculations, can vary by as much as a factor of three.

On the other hand, recent calculations of the transport properties of strongly correlated systems using dynamical mean-field theory¹ to solve the Hubbard model on a frustrated hypercubic lattice, indicate that as the electronic correlations become stronger there is a clear crossover from a Fermi liquid at low temperatures to a “bad metal” with no quasiparticles at high temperatures. However, such a crossover and the associated signatures in transport properties (e.g., a peak in the temperature dependence of the thermopower and resistivity, and disappearance of the Drude peak in the optical conductivity) are only observed for sufficiently large values of the ratio: $m_c^*/m_c \sim 3 - 4$. For smaller values, transport properties resemble the ones found in a nearly free-electron metal. Since the transport

properties of the organic metals do show the signatures discussed above it is important to have accurate estimates of m^*/m_c in order to check the consistency of describing them as strongly correlated systems.

In this paper, we show that in a quasi-two-dimensional Fermi liquid there is a simple relation between the cyclotron mass and the density of states at the Fermi surface. This result, Eq. (7), holds for *any* dispersion relation for the quasiparticles. Using this relation, we compute the ratio of the cyclotron band masses associated with the α and β orbits, m_c^β/m_c^α , for a model band structure for κ -(BEDT-TTF)₂X. The ratio is approximately 2, and varies by only about ten per cent even when the band structure parameters are varied significantly. This is in good agreement with values of $m^{*\beta}/m^{*\alpha}$, deduced from magnetic oscillation experiments, suggesting that the quasiparticle renormalisation factor does not vary significantly between different parts of the Fermi surface.

B. Different effective masses

We now briefly review several of the effective masses which can be defined for electrons or quasiparticles with a general dispersion relation $\epsilon(\mathbf{k})$.

Band mass tensor. This is defined as⁵

$$m_{\nu\mu}^b \equiv \hbar^2 \left(\frac{\partial^2 \epsilon(\mathbf{k})}{\partial k_\nu \partial k_\mu} \right)^{-1} \quad (2)$$

where ν and μ are Cartesian coordinates, and gives information of the band dispersion for any value of the electronic momentum. In particular, from the band mass tensor, the band dispersion of the electrons in *all* directions near the Fermi surface can be reconstructed.

Cyclotron mass. When a metal is in the presence of an external magnetic field the electrons undergo periodic orbits in both position and momentum space. The cyclotron frequency, ω_c , associated with the periodic motion along these orbits on the Fermi surface is given by⁶

$$\frac{1}{\omega_c} = \frac{\hbar^2}{2\pi e B} \oint \frac{dk}{(\nabla \epsilon(\mathbf{k}))_\perp} \equiv \frac{m_c}{eB} \quad (3)$$

where B is the strength of the magnetic field and $(\nabla \epsilon(\mathbf{k}))_\perp$, is the gradient of the dispersion relation in the plane perpendicular to the field and the line integral is around the periodic orbit on the Fermi surface. The last relation has been used to define a cyclotron effective mass, m_c . Note that this effective mass involves an average of the dispersion relation along the periodic orbit. It determines the energy spacing of the Landau levels and can be extracted from the temperature dependence of the amplitude of magnetic oscillations, as discussed above.

Plasma frequencies. Reflectivity measurements can be used to determine the plasma frequency associated with collective oscillations of a charged Fermi liquid. Polarized light can be used to determine the anisotropy of these frequencies. For light polarized with the electric field in the μ direction in a metal with Fermi energy ϵ_F , the plasma frequency, $\omega_{p\mu}$, is given by,⁷

$$\omega_{p\mu}^2 = \left(\frac{e}{\pi \hbar} \right)^2 \int d^3 \mathbf{k} \frac{\partial^2 \epsilon(\mathbf{k})}{\partial k_\mu^2} \theta(\epsilon_F - \epsilon_{\mathbf{k}}) \equiv \frac{n e^2}{m_{p\mu}} \quad (4)$$

where the integral runs over the first Brillouin zone and the last identity has been used to define an effective mass, $m_{p\mu}$, when n is the total number of charge carriers. The above expression is derived from Lindhard's dielectric function. Note that in contrast with the cyclotron mass in Eq. (3), which depends on electron states at the Fermi surface, the plasma mass includes all the occupied states, and not only those which are close to the Fermi energy. This is because the plasma oscillation is a collective process in which all the electrons participate.

For a parabolic dispersion relation, $\epsilon(\mathbf{k}) = \hbar^2 k^2 / (2m_0)$, all of the effective masses defined above will equal m_0 . However, we stress that for a general dispersion relation they will *not* be equal and so caution is in order when trying to compare effective masses extracted from different measurements.

C. The cyclotron mass and the density of states

We now show how for a quasi-two-dimensional metal, the cyclotron mass defined by (3) is simply related to the density of states at the Fermi energy. First, following Ashcroft and Mermin,⁶ Eq. (3) can be rearranged to give

$$m_c = \frac{\hbar^2}{2\pi} \frac{\partial A(\epsilon_F)}{\partial \epsilon_F} \quad (5)$$

where $A(\epsilon_F)$ is the area of the cross section of the Fermi surface defined by the orbit described by an electron or hole, in the presence of a the magnetic field, B .

For a quasi-two-dimensional system with only one band that crosses the Fermi energy, and a magnetic field perpendicular to the layers, the area of the orbit is just the cross sectional area of the Fermi surface within a layer

$$A(\epsilon_F) = 4\pi^2 \sum_{\mathbf{k}} \theta(\epsilon_F - \epsilon(\mathbf{k})) \quad (6)$$

where \mathbf{k} is the two-dimensional wavevector within a layer. Eq.(6) is just based on state counting and assumes that the interlayer dispersion can be neglected. Corrections due to a finite interlayer bandwidth will be of order t_c/ϵ_F where t_c is the interlayer hopping integral. For typical organic metals this ratio is less than 0.01.^{3,8} Taking the derivative of (6) with respect to ϵ_F gives, for the cyclotron mass

$$m_c = 2\pi\hbar^2 \rho_\sigma(\epsilon_F) \quad (7)$$

where $\rho_\sigma(\epsilon_F)$ is the density of states per spin at the Fermi energy, $\rho_\sigma(\epsilon_F) = \sum_{\mathbf{k}} \delta(\epsilon_F - \epsilon(\mathbf{k}))$. We stress that this simple expression for the cyclotron band mass is only true for quasi-two-dimensional metals. In other cases, the reduction of the general expression (5) to (7) cannot be done. For example, for a three-dimensional system the area associated to an electron or hole orbit is not defined by Eq. (6), and, therefore, it is not possible to relate the cyclotron mass to the density of states at the Fermi energy. The result (7) was previously pointed out by Tamura *et al.*⁹ but its significance appears to have been completely overlooked. We will show below that as a consequence of Luttinger's theorem it is also true in the presence of interactions.

For more general situations where the Fermi surface of the metal crosses several bands, the different cyclotron masses can be expressed in terms of the partial density of states associated with each of the bands. As an example, we will compute the band cyclotron masses for the α and β orbits in the κ -(BEDT-TTF)₂X family, for which several bands are present.

D. Model band structures

There are several approaches used for calculating the band structure of layered materials. Semi-empirical approaches such as the Hückel approximation use parametrized tight-binding Hamiltonians with parameters that are partially determined from experiment. In the case of κ -(BEDT-TTF)₂X crystals, the effective tight-binding Hamiltonian which is used to model the interaction between the antibonding orbitals of BEDT-TTF dimers is^{10–12,2}

$$H = t_1 \sum_{ij} (c_i^\dagger c_j + h.c.) + t_3 \sum_{ik} (c_i^\dagger c_k + h.c.) + t_2 \sum_{il} (c_i^\dagger c_l + h.c.) \quad (8)$$

where c_i^\dagger , creates an electron in the antibonding orbital at site i on a square lattice. t_1 and t_3 are nearest-neighbour hoppings, and t_2 is the next-nearest neighbour hopping amplitude along only *one* diagonal. The κ -(BEDT-TTF)₂X materials have two dimers per unit cell and, because t_1 and t_3 can be slightly different the two dimers in each cell of the κ -(BEDT-TTF)₂X materials are inequivalent. The relationship between the different hopping integrals and the geometrical arrangement of the BEDT-TTF molecules is shown in Fig. 1.

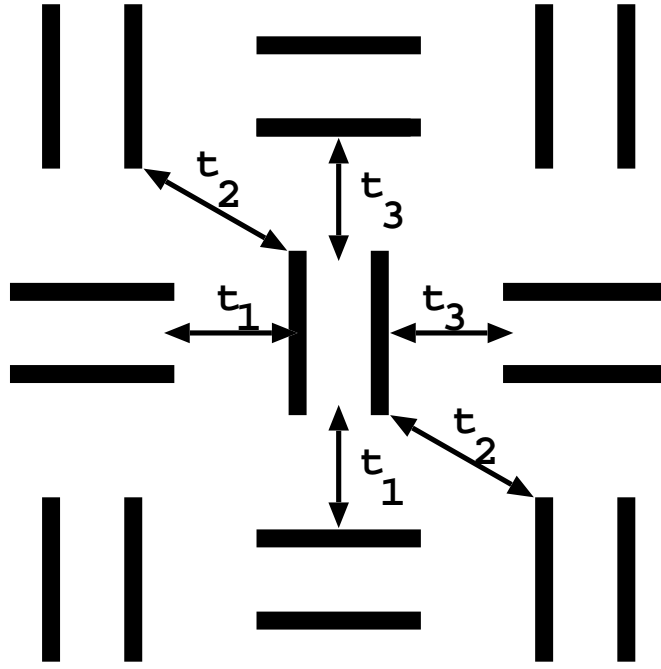


FIG. 1. Stacking pattern of the BEDT-TTF molecules within a layer of the κ -(BEDT-TTF) $_2$ X family of organic metals. t_1 , t_2 and t_3 denote hopping amplitudes between *dimers* of molecules.

In Fig. 2 we show the stacking pattern for the β -(BEDT-TTF) $_2$ X family. In this case all the sites in the lattice are equivalent and there is only one dimer per unit cell.

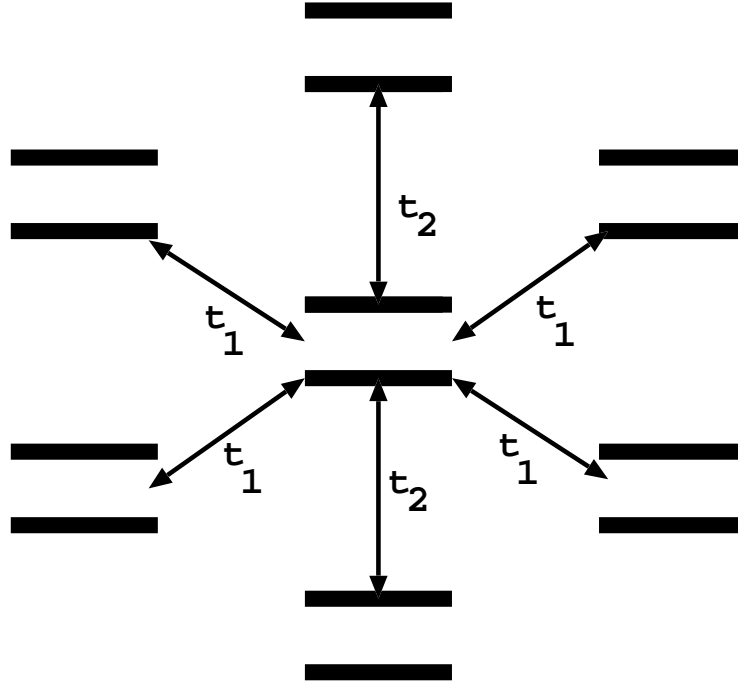


FIG. 2. Stacking pattern of the BEDT-TTF molecules within a layer of the β -(BEDT-TTF) $_2$ X family of organic superconductors. t_1 and t_2 denote hopping amplitudes between *dimers* of molecules.

If we diagonalize the Hamiltonian (8), we obtain the two dispersion relations

$$\epsilon^\pm(\mathbf{k}) = t_2 \cos(k_y) \pm (t_1^2 + t_3^2 + 2t_1 t_3 \cos(k_x))^{1/2} \cos(k_y/2) \quad (9)$$

The Fermi surface is shown in Fig. 3, for $t_1 - t_3 = 0.05$ and $t_2 = t_1$. The α orbit is associated with the hole pocket in

the Fermi surface and the unoccupied part of the lower band, $\epsilon(\mathbf{k})$, while the β orbit (which occurs in large magnetic fields due to magnetic breakdown) contains parts from both the upper and lower band dispersions and corresponds to the outer orbit described with arrows in Fig. 3.

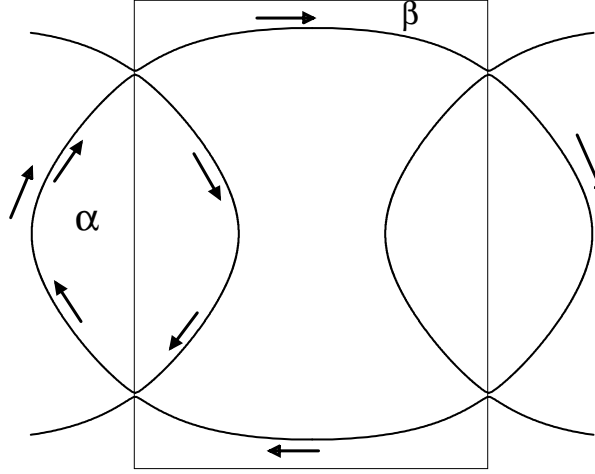


FIG. 3. α and β orbits on the intralayer Fermi surface in a κ -(BEDT-TTF) $_2$ X material. The arrows indicate the motion of holes on each orbit in the presence of a magnetic field perpendicular to the layers. The box determines the Brillouin zone boundary. There is a small energy gap at the boundary and the β orbit is only observed in magnetic oscillations due to magnetic breakdown. In the β -(BEDT-TTF) $_2$ X family the Brillouin zone is twice as large and there is no α orbit.

For the β -(BEDT-TTF) $_2$ X materials, due to the columnar stacking of the BEDT-TTF molecules and being $t_1 \sim t_2 \sim t_3$, there is only one dimer of BEDT-TTF molecules per site, and there is only one half-filled band which cuts the Fermi energy and is described by

$$\epsilon(\mathbf{k}) = t_2 \cos(k_y) + 2t_1 \cos(k_x/2) \cos(k_y/2) \quad (10)$$

For the θ -(BEDT-TTF) $_2$ X materials, the geometrical arrangement is similar to that for κ -(BEDT-TTF) $_2$ X with each dimer replaced by a single BEDT-TTF molecule.¹³ It is then described by the dispersion relation (9) but the band is 3/4 filled.

We have evaluated the cyclotron band masses associated with the different orbits described along the Fermi surface for κ -(BEDT-TTF) $_2$ X. The area associated with the α -orbit (see Fig. 3) is given by

$$A^\alpha(\epsilon_F) = 4\pi^2 \sum_{\mathbf{k}} (1 - \theta(\epsilon_F - \epsilon^-(\mathbf{k}))) \quad (11)$$

and the cyclotron effective mass is, from Eq. (7)

$$m_c^\alpha = 2\pi\hbar^2 \rho_\sigma^-(\epsilon_F) \quad (12)$$

where $\rho_\sigma^-(\epsilon_F)$, is the density of states per unit cell and spin associated with the $\epsilon^-(\mathbf{k})$ band. Similarly, the area enclosed by the β -orbit is

$$A^\beta(\epsilon_F) = 4\pi^2 \sum_{\mathbf{k}} (1 - \theta(\epsilon_F - \epsilon^+(\mathbf{k}))) + 4\pi^2 \sum_{\mathbf{k}} (1 - \theta(\epsilon_F - \epsilon^-(\mathbf{k}))) \quad (13)$$

and the cyclotron mass is proportional to the total density of states:

$$m_c^\beta = 2\pi\hbar^2 \rho_\sigma(\epsilon_F) \quad (14)$$

where $\rho_\sigma(\epsilon_F)$ is the total density of states per unit cell and spin. Note that a minus sign comes in the above expressions when we are considering the electron mass instead of the hole mass as $m_e = -m_h$, where m_h is the hole mass.

For the dispersion (9) with $t_1 = t_2 = t_3 = t$, Ivanov, Yakushi, and Ugolkova¹⁴ have obtained analytical expressions for the density of states projected onto the upper and lower bands can be obtained. If all energies are in units of t , the total density of states per unit cell and spin is

$$\begin{aligned}\rho(-3/2 \leq \epsilon \leq -1) &= \frac{2}{\pi^2 q \sqrt{\tau}} K\left(\frac{1}{q}\right) \\ \rho(-1 \leq \epsilon \leq 3) &= \frac{2}{\pi^2 \sqrt{\tau}} K(q)\end{aligned}\tag{15}$$

and, for the partial density of states associated with the lower band

$$\begin{aligned}\rho^-\left(\frac{-3}{2} \leq \epsilon \leq -1\right) &= \frac{2}{\pi^2 q \sqrt{\tau}} K\left(\frac{1}{q}\right) \\ \rho^-(-1 \leq \epsilon \leq 1) &= \frac{2}{\pi^2 \sqrt{\tau}} F\left(\arcsin\left(\frac{1}{2q} \sqrt{\frac{(5-\tau^2)(\tau+1)}{2}}\right); q\right)\end{aligned}\tag{16}$$

where $q = \sqrt{1 - (\tau - 1)^3(\tau + 3)/(16\tau)}$ with $\tau = \sqrt{2\epsilon + 3}$. K and F are the complete elliptic integral and the elliptic integral of the first kind, respectively.

From the above expressions and Eq. (7) we obtain the following cyclotron masses: $m_c^\beta/m_e = 0.23/t$ and $m_c^\alpha/m_e = 0.11/t$, with t given in eV and we have used the intralayer unit cell area of $A = 104 \text{ \AA}^2$. This gives $m_c^\beta/m_c^\alpha = 2$ and it turns out that this ratio is relatively insensitive to variations in the band structure parameters. We have relaxed the condition on the hopping integrals $t_1 = t_2 = t_3$, and, we have numerically evaluated the partial density of states instead of using eq.(15) and eq.(16). The ratio of the cyclotron masses obtained from the effective dimer model for fixed $t_1 = t_3$ but different values of t_2/t_1 is, $m_c^\beta/m_c^\alpha = 2.4, 2.2$, and 2.0 , for $t_2/t_1 = 0.5, 0.7, 1.0$, respectively.

In order to have a realistic description of the layered materials we use the hopping amplitudes obtained from quantum chemistry calculations using the Hückel approximation and, in some cases, results obtained from first-principle calculations. The hoppings of the effective dimer model, for which $t_1 = t_3$ and $t_1 \neq t_2$, are given in Table I. A more detailed discussion of this model and the relationship between t_1 and t_2 and the intermolecular hoppings calculated in the Hückel approximation can be found in Reference 2. A minor point is that if we denote the Coulomb repulsion in each molecule by U_0 , and the hopping amplitude between the molecules within one dimer by t_b , for $U_0 \gg 4t_b$ (strongly correlated case), the hopping amplitudes should be corrected by a factor of $1/\sqrt{2}$ with respect to the ones obtained from the Hückel calculation. However, in the case $U_0 \sim 4t_b$, this factor is 0.92 and the effect of correlations to the matrix elements is small. Different calculations suggest that the ratio $U_0/4t_b \sim 1$, so that in Table I we multiply all the bare hoppings by 0.92.

In Table I, we also give the cyclotron masses obtained from eq.(7), where the density of states has been computed numerically for the different hoppings. It can be seen that the calculated cyclotron band masses are sensitive to the parameters and the values deduced from the parameters calculated by different groups for the same material can vary significantly. However, the calculated ratio, m_c^β/m_c^α , is relatively insensitive to the parameters.

The band structures of the (BEDT-TTF)₂X family have been calculated by several different techniques and some of the results for the density of states at the Fermi energy are compared in Table II. The Hückel method is the simplest and only considers the π orbitals and neglects all σ orbitals. The overlap integrals that are calculated are all scaled by some empirical parameter and then used as hopping integrals in a tight-binding band structure. It is generally acknowledged that this method gives a good qualitative description of electronic properties (such as the symmetry and ordering of states) but cannot give a quantitative description of electronic properties.¹⁵

The extended Hückel method¹⁶ treats both π and σ orbitals. Although it is more quantitatively reliable than the Hückel approximation it still does not give a completely quantitative description of organic molecules. It has been used to calculate the band structure of a wide range of organic metals by Whangbo and coworkers¹⁷.

The energy levels for a pair of BEDT-TTF dimers with the same geometrical arrangement as in κ -(BEDT-TTF)₂Cu[N(CN)₂]Br have been calculated by an *ab initio* method. The tight-binding parameters for a Hubbard model for the dimers is then evaluated by fitting the energy levels to the *ab initio* values. The resulting parameters are similar to those obtained by an extended Hückel calculation for the dimer pair.¹⁸ But the resulting density of states is more than twice the results of extended Hückel for the solid.

The most reliable method of calculating band structures is generally considered to be *ab initio* methods based on the local density approximation (LDA). Nevertheless, different groups still often obtain quite different results. For example, values obtained for the density of states at the Fermi energy in the fullerene metal, K₃C₆₀, differ by as much

as fifty per cent.¹⁹ (Extended Hückel calculations do fall in this range). Due to the large number of atoms in a unit cell only a few *ab initio* calculations have been attempted for the (BEDT-TTF)₂X materials.

Results for the density of states (and the corresponding cyclotron masses) obtained using the three methods are shown in Table II. Note the large variation in results for each of the materials. In particular, the Hückel method gives masses that are two to five times larger than those obtained by the other more sophisticated methods.

E. The cyclotron mass in the presence of interactions

The above treatment neglected the effect of interactions between the electrons. We now show that Eq. (7) has a natural generalization in the case of a Fermi liquid. The one-electron Green's function in a general interacting electron system is

$$G(\mathbf{k}, \omega + i\eta) = \frac{1}{\omega + i\eta - \epsilon(\mathbf{k}) - \Sigma(\mathbf{k}, \omega)} \quad (17)$$

in momentum space, where $\Sigma(\mathbf{k}, \omega)$ is the electron self-energy. In a Fermi liquid, near the quasiparticle poles, the Green's function can be rewritten as

$$G(\mathbf{k}, \omega) = \frac{Z_{\mathbf{k}}}{\omega - \tilde{\epsilon}(\mathbf{k})} \quad (18)$$

where $\tilde{\epsilon}(\mathbf{k})$ is the quasiparticle energy and $Z_{\mathbf{k}} = \frac{1}{1 - \frac{\partial \Sigma(\mathbf{k}, \omega)}{\partial \omega}|_{\omega=\tilde{\epsilon}(\mathbf{k})}}$ is the residue at the quasiparticle pole. Note that the above expression is true for a Fermi liquid, and for electrons with momentum close to the Fermi surface for which $\text{Im}\Sigma(\mathbf{k} \rightarrow \mathbf{k}_F, \omega \rightarrow \epsilon_F) \rightarrow 0$. The spectral density is then given by

$$A(\mathbf{k}, \omega) = -\frac{1}{\pi} \text{Im}G(\omega + i\eta) = \frac{\delta(\omega - \tilde{\epsilon}(\mathbf{k}))}{1 - \frac{\partial \Sigma(\mathbf{k}, \omega)}{\partial \omega}|_{\omega=\tilde{\epsilon}(\mathbf{k})}} \quad (19)$$

Thus, the quasiparticle density of states at the Fermi energy is

$$\tilde{\rho}(\tilde{\epsilon}_F) = \sum_{\mathbf{k}} \delta(\tilde{\epsilon}_F - \tilde{\epsilon}(\mathbf{k})) = \sum_{\mathbf{k}} \left(1 - \frac{\partial \Sigma(\mathbf{k}, \omega)}{\partial \omega}|_{\omega=\tilde{\epsilon}_F}\right) A(\mathbf{k}, \tilde{\epsilon}_F) \quad (20)$$

Müller-Hartman²⁰ showed that, if the self energy is independent of momentum, then at zero temperature, $\sum_{\mathbf{k}} A(\mathbf{k}, \tilde{\epsilon}_F) = \rho(\epsilon_F)$, the non-interacting density of states at the Fermi energy. So in this case, $\tilde{\rho}(\tilde{\epsilon}_F) = \rho(\epsilon_F)/Z$. Note that the quasiparticle density of states is always enhanced because for a Fermi liquid $\frac{\partial \Sigma(\mathbf{k}, \omega)}{\partial \omega}|_{\omega=\tilde{\epsilon}_F} < 0$.

Some time ago, Luttinger²¹ showed that in an interacting system with Fermi liquid properties, the results of Lifshitz and Kosevich still describe the de Haas van Alphen oscillations provided that the relevant quasiparticle quantities are used. Thus, (5) is replaced by $m_c^* = \frac{\partial \tilde{A}}{\partial \tilde{\epsilon}_F}$ where a tilde denotes renormalised quantities. In a quasi-two-dimensional Fermi liquid, the area enclosed by the orbits of the quasiparticles is

$$\tilde{A}(\tilde{\epsilon}_F) = 4\pi^2 \sum_{\mathbf{k}} \theta(\tilde{\epsilon}_F - \tilde{\epsilon}(\mathbf{k})) \quad (21)$$

and so, we find that the cyclotron effective mass is

$$m_c^* = 2\pi\hbar^2 \sum_{\mathbf{k}} \delta(\tilde{\epsilon}_F - \tilde{\epsilon}(\mathbf{k})) = 2\pi\hbar^2 \tilde{\rho}_\sigma(\tilde{\epsilon}_F) \quad (22)$$

Again, equations (22) and (20) show the cyclotron mass enhancement produced by the factor appearing in eq.(20). The same enhancement also appears in the specific heat coefficient.²² A further simplification is obtained for the case of a momentum independent self-energy, as then the cyclotron effective masses reduce to

$$m_c^* = 2\pi^2\hbar^2 \rho(\epsilon_F)/Z = m_c/Z \quad (23)$$

where Z is the quasiparticle weight, which, in terms of the self-energy, is: $Z = (1 - \frac{\partial \Sigma(\omega)}{\partial \omega}|_{\omega=\tilde{\epsilon}_F})^{-1}$. In this case, the ratios of the cyclotron effective masses associated with the quasiparticles moving along different orbits, $m_c^{*\beta}/m_c^{*\alpha}$, should be the same as the ratios associated with the non-interacting system, m_c^β/m_c^α .

A partial test of the momentum independent self energy is provided by comparing the measured ratios of the renormalized cyclotron masses in different orbits with the cyclotron band mass ratios. This is done in Table I. The relative consistency between the observed values of this ratio and the band structure values suggests that if there are sizeable renormalizations due to many-body effects then these renormalizations are not significantly different on the different parts of the Fermi surface. However, this consistency is only a necessary condition but not sufficient for having a momentum independent self energy, as cyclotron masses include averages over the Fermi surface and, therefore, cancellations of contributions from different parts of the Fermi surface may occur.

Furthermore, in Reference 10 the effective masses for κ -(BEDT-TTF)₂Cu(SCN)₂ were measured as the pressure was increased from 1 bar to 20 kbar. $m_c^{*\beta}/m_e$ decreased from 6.5 ± 0.1 at 1 bar to 2.7 ± 0.1 at 16.3 kbar. $m_c^{*\alpha}/m_e$ decreased from 3.5 ± 0.1 at 1 bar to 1.4 ± 0.1 at 16.3 kbar. However, the ratio $m_c^{*\beta}/m_c^{*\alpha}$ has a constant value of 1.9 within error.

F. Specific heat

Measurements of the electronic specific heat in the (BEDT-TTF)₂X crystals and Sr₂RuO₄ show a linear temperature dependence at low temperatures, consistent with a Fermi liquid description. The corresponding specific heat coefficient γ is given in Table III for some of these materials. This coefficient is related to the quasiparticle density of states at the Fermi energy, $\tilde{\rho}(\tilde{\epsilon}_F)$, (see Eq. (20)) by

$$\gamma = \frac{2\pi^2 k_B^2}{3} \tilde{\rho}(\tilde{\epsilon}_F) \quad (24)$$

Since the quasiparticle density of states is also related to the cyclotron effective mass by Eq. (22) the measured specific heat coefficient can be used to calculate a corresponding cyclotron effective mass. This has been done in Table III for a range of organic materials. The values obtained for $m_c^{*\beta}/m_e$ from specific heat measurements agree for κ -(BEDT-TTF)₂I₃ and β -(BEDT-TTF)₂I₃ but not for the materials with copper in the anion. Since this comparison does provide a quantitative test of a Fermi liquid description further careful measurements are justified, particularly on a wider range of materials.

Such a comparison was also done recently for Sr₂RuO₄ in Reference 4, where relation (22) was implicitly assumed, presumably based on its validity for a parabolic dispersion relation. Our work provides a rigorous justification for this comparison. In Sr₂RuO₄ there are three distinct Fermi surfaces and the associated cyclotron masses deduced from de Haas van Alphen oscillations were $m_c^*/m_e=3.4, 7.5$ and 14.6 for the α, β and γ orbits, respectively.²³ From the above discussion, it follows that the specific heat coefficient of Sr₂RuO₄ is related to the effective masses by

$$\gamma = \frac{\pi k_B^2}{3\hbar^2} (m_c^{*\alpha} + m_c^{*\beta} + m_c^{*\gamma}) \quad (25)$$

which comes from the fact that the total density of states is just the sum of the density of states of the different Fermi surfaces. Evaluating (25) we obtain a specific heat coefficient of $36.7 \text{ mJ}/(\text{K}^2 \text{ mol})$, which agrees with the measured value²⁴ of $37.4 \text{ mJ}/(\text{K}^2 \text{ mol})$.

G. Conclusions

We now summarize our results and their implications. First, it was shown that in a quasi-two-dimensional metal in which the dispersion perpendicular to the layers can be neglected, the cyclotron effective mass for a particular orbit in a general band structure is simply related to the density of states at the Fermi energy associated with the relevant band. Second, it was shown that, due to Luttinger's results for a Fermi liquid, a similar relationship holds in the presence of interactions.

These results have a number of general applications to layered metals which have Fermi liquid properties at low temperatures.

(i) In order to evaluate the effective mass from band structure it is not necessary to numerically evaluate the derivative in (5), as has been done previously by a number of authors. Instead (7) can be used together with the density of states at the Fermi energy. This eliminates the need to perform the cumbersome task of repeating the band structure calculations for many different Fermi energies.

(ii) We found that for model band structures describing the family κ -(BEDT-TTF)₂X, the ratio of the effective mass for the β -orbit to the mass for the α orbit is fairly insensitive to the details of the band structure, having a value close to two.

(iii) Our results imply that a quantitative test of the Fermi liquid description of a layered metal is to compare measurements of the cyclotron effective mass to the linear coefficient in the specific heat.

(iv) The agreement between the ratio of the different measured cyclotron masses and the ratio calculated from band structure, suggests a momentum independent self-energy, although other experimental probes such as polarized Raman scattering, photoemission spectra, and angular dependent magnetoresistance oscillations are needed before making any definitive conclusion.

Based on comparison with a wide range of materials we conclude the following. First, the effective masses deduced from magnetic oscillations and specific heat are consistent for Sr_2RuO_4 and for two out of four of the organic materials considered. For three out of four of the organic materials for which data is available the measured ratio $m_c^{*\beta}/m_c^{*\alpha}$ is consistent with the band structure ratio m_c^β/m_c^α . Furthermore, for the $\kappa\text{-(BEDT-TTF)}_2\text{Cu(NCS)}_2$ this ratio does not change under pressure while the individual effective masses decrease by a factor of 2.5. This suggests that the self energy does not vary significantly over the different parts of the Fermi surface. We also note that the significant variation of the effective masses with pressure cannot be explained in terms of band structure; it predicts a small variation with pressure.

A comparison of the results of band structure calculations using a range of methods found that they produced a large range in values for the density of states (and thus the effective masses). The Hückel method has often been used to estimate the hopping integrals in tight binding band structures (as in Table I). It is less sophisticated than the extended Hückel method which in turn is less sophisticated than *ab initio* methods based on the local density approximation. We suggest that the Hückel method is producing hopping integrals which are too small by a factor of two to four. The best strategy to evaluate these integrals would be to fit a LDA band structure to a tight binding dispersion, such as (9). Such an approach was recently taken for Sr_2RuO_4 .²⁵

We now come back to the central question of this paper: are the layered metals we have considered strongly correlated? A definitive answer is not possible because of the large variation in values for the band cyclotron masses that have been calculated by different band structure methods. However, we suggest that due to their greater sophistication, the local density approximation and extended Hückel approximation calculations give the most reliable values. We suggest that the appropriate values for the band cyclotron masses are those calculated by the local density approximation and extended Hückel approximation. The mass ratios given in Table II then imply that $m_c^{*\beta}/m_c \sim 2.5 - 4$, suggesting appreciable quasiparticle renormalization due to many-body effects. This is consistent with the strong temperature dependence of the transport properties, discussed in detail in Reference 1.

TABLE I. Cyclotron effective masses predicted by tight-binding band structures with values of the hopping integrals given by different Hückel calculations. EHA denotes the extended Hückel approximation. These masses are compared to values deduced from magnetic oscillation experiments. The cyclotron masses are obtained from Eq. (7) with the density of states computed from the tight-binding Hamiltonian (8) for the given values of the hopping integrals t_1 and t_2 and with $t_1 = t_3$. Note that the ratio of the masses for the β and α orbits in Figure 3 depends weakly on the band structure parameters. Except for the second line, all the results are for ambient pressure.

	t_1 (meV)	t_2 (meV)	Ref	m_c^β/m_e	$m_c^{*\beta}/m_e$ (expt)	m_c^β/m_c^α	$m_c^{*\beta}/m_c^{*\alpha}$ (expt)
κ -(BEDT-TTF) ₂ Cu(SCN) ₂	31.3	23.0	26	8.5	6.5^{10}	2.2	1.9^{10}
7.4 kbar	40.5	24.8	26	7.4	$\sim 3.5^{27}$	2.3	~ 2.0
κ -(BEDT-TTF) ₂ Cu[N(CN) ₂]Br	61.7	32.7	18	4.6	6.4^{28}	2.35	?
	62.1	42.3	29	4.4	6.4^{28}	2.2	?
ab initio	78.2	39.0	18	3.8	6.4^{28}	2.35	?
κ -(BEDT-TTF) ₂ Cu ₂ (CN) ₃	50.1	53.0	29	4.6	4.0^{30}	2.0	?
κ -(BEDT-TTF) ₂ I ₃	70.0	40.5	29	4.1	3.9^3	2.3	2.0
	54.0	34.0	31	5.3	3.9^3	2.3	2.0
κ -(BETS) ₂ GaCl ₄	?	?		?	5.3^{32}	?	1.6
κ -(BETS) ₂ C(CN) ₃	EHA	?	33	1.2	3.3^{33}	?	1.9
θ -(BEDT-TTF) ₂ I ₃	42.0	64.0	34	2.2	3.6^9	2.6	1.8
β -(BEDT-TTF) ₂ I ₃	60.0	42.0	35	4.3	4.2^{36}	-	-

TABLE II. Comparison of the density of states at the Fermi energy (and the associated effective masses) which is obtained from different methods of calculating band structure. LDA denotes *ab initio* calculations using the local density approximation. EHA denotes the extended Hückel approximation and HA denotes values from Table I, based on the Hückel approximation. The cyclotron masses are calculated from the density of states using Eq. (7). The density of states $\rho(\epsilon_F)$ is given in units of states per unit cell per spin per eV. Note that the Hückel method gives effective masses that are two to five times larger than the other more sophisticated methods.

	LDA		EHA		HA		Expt
	$\rho(\epsilon_F)$	m_c^β/m_e	$\rho(\epsilon_F)$	m_c^β/m_e	$\rho(\epsilon_F)$	m_c^β/m_e	$m_c^{*\beta}/m_e$
κ -(BEDT-TTF) ₂ Cu(SCN) ₂	6.4^{37}	2.6	4.2^{38}	1.7	21.2	8.5	6.5
κ -(BEDT-TTF) ₂ Cu[N(CN) ₂]Br	6.9^{39}	2.7	4.4^{38}	1.7	11.7	4.6	6.4
β -(BEDT-TTF) ₂ I ₃	?		3.1^{38}	1.6	5.6	4.3	4.2

TABLE III. Comparison of the cyclotron effective masses, $m^{*\beta}$, deduced from the measurements of magnetic oscillations associated with the β orbit and the masses deduced from the linear specific heat coefficient γ and equations (7) and (24). A is the area of the unit cell within a layer and m_e is the free electron mass.

	$A(\text{\AA}^2)$	$m^{*\beta}/m_e$	$\gamma(\text{mJ}/(\text{K}^2 \text{ mol}))$	$m^*/m_e(\gamma)$
κ -(BEDT-TTF) ₂ Cu(SCN) ₂	104.0	6.5 ± 0.1^{10}	25 ± 3^{40}	4.4 ± 0.5
κ -(BEDT-TTF) ₂ Cu[N(CN) ₂]Br	108.6	$5.4^{41}, 6.4^{28}$	$22 \pm 3^{42}, 25 \pm 2^{43}$	4 ± 1
κ -(BEDT-TTF) ₂ I ₃	103.0	3.9^3	19 ± 1.5^{44}	3.4 ± 0.3
β -(BEDT-TTF) ₂ I ₃	56.3	4.2 ± 0.2^{36}	24 ± 3^{45}	3.9 ± 0.5

ACKNOWLEDGMENTS

We thank R. McKinnon, N. Harrison, J. S. Brooks, J. Wosnitzer, and E. Canadell for helpful discussions. This work was supported by the Australian Research Council.

* e-mail: merino@phys.unsw.edu.au

** e-mail: ross@phys.unsw.edu.au

- ¹ J. Merino and R. H. McKenzie, cond-mat/9909041, to appear in Phys. Rev. B, March 15.
- ² R. H. McKenzie, Comments Cond. Mat. Phys. **18**, 309 (1998).
- ³ J. Wosnitzer, *Fermi Surface of Low-Dimensional Organic Metals and Superconductors*, Springer-Verlag, Berlin-Heidelberg (1996).
- ⁴ A. P. Mackenzie, S. R. Julian, A. J. Diver, G. J. McMullan, M. P. Ray, G. G. Lonzarich, Y. Maeno, S. Nishizaki and T. Fujita, Phys. Rev. Lett. **76**, 3786 (1996).
- ⁵ C. Kittel, *Introduction to Solid State Physics*, 7th ed. (Wiley, New York, 1996).
- ⁶ N. Ashcroft and Mermin, *Solid State Physics* (Saunders, Philadelphia, 1976), p. 231-233.
- ⁷ J. F. Kwak, Phys. Rev. B **26**, 4789 (1982).
- ⁸ P. Moses and R.H. McKenzie, Phys. Rev. B **60**, 7998 (1999)
- ⁹ M. Tamura, H. Kuroda, S. Uji, H. Aoki, M. Tokumoto, A. G. Swanson, J. S. Brooks, C. C. Agosta and S. T. Hannahs, J. Phys. Soc. Japan **2**, 615 (1994).
- ¹⁰ J. Caulfield, W. Lubczynski, F. L. Pratt, J. Singleton, D. Y. Ko, W. Hayes, M. Kurmoo, and P. Day, J. Phys. Condens. Matter **6** 2911 (1994).
- ¹¹ G. Visentini, A. Painelli, A. Girlando, and A. Fortunelli, Europhys. Lett. **42**, 467 (1998).
- ¹² H. Kino and H. Fukuyama, J. Phys. Soc. Jap. **65**, 2158 (1996).
- ¹³ H. Mori *et al.*, Phys. Rev. B **57**, 12023 (1998)
- ¹⁴ V. Ivanov, K. Yakushi, and E. Ugolkova, Physica C **275** 26 (1997).
- ¹⁵ For a review see, J. P. Lowe, *Quantum Chemistry* (Academic, New York, 1978).
- ¹⁶ M. H. Whangbo and R. Hoffman, J. Am. Chem. Soc. **100**, 6093 (1978).
- ¹⁷ J. M. Williams *et al.*, *Organic superconductors (including fullerenes) : synthesis, structure, properties, and theory* (Prentice Hall, Englewood Cliffs, 1992), and references therein.
- ¹⁸ A. Fortunelli and A. Painelli, J. Chem. Phys. **106**, 8051 (1997).
- ¹⁹ O. Gunnarsson, Rev. Mod. Phys. **69**, 575 (1997). Table V.
- ²⁰ E. Müller-Hartmann, Z. Phys. B **74**, 507 (1989).
- ²¹ J. M. Luttinger, Phys. Rev. **121**, 1251 (1961).
- ²² J. M. Luttinger, Phys. Rev. **119**, 1153 (1960); A non-perturbative proof of Luttinger's theorem can be found in M. Oshikawa, cond-mat/0002392.
- ²³ The masses given in Ref. 4 are corrected in Ref. 24.
- ²⁴ A. P. Mackenzie *et al.*, J. Phys. Soc. Japan **67**, 385 (1998).
- ²⁵ I. I. Mazin, D. A. Papaconstantopoulos, and D. J. Singh, cond-mat/9907442.
- ²⁶ M. Rahal, D. Chasseau, J. Gaultier, L. Ducasse, M. Kurmoo, and P. Day, Acta Cryst. B **53**, 159 (1997).
- ²⁷ This value was estimated by interpolating values given in Ref. 10 for different pressures.
- ²⁸ H. Weiss *et al.*, JETP Lett. **66**, 202 (1997).
- ²⁹ T. Komatsu *et al.*, J. Phys. Soc. Japan **65**, 1340 (1996).
- ³⁰ E. Ohmichi, H. Ito, T. Ishiguro, G. Saito and T. Komatsu, Phys. Rev. B **57**, 7481 (1998).
- ³¹ M. Tamura, H. Tajima, K. Yakushi, H. Kuroda, A. Kobayashi, R. Kato and H. Kobayashi, J. Phys. Soc. Japan **60**, 3861 (1991).
- ³² S. I. Pesotskii, R. B. Lyubovskii, N. D. Kushch, M. V. Kartsovnik, W. Biberacher, K. Andres, H. Kobayashi, and A. Kobayashi, JETP **88**, 114 (1999).
- ³³ B. Zh. Narymbetov, N. D. Kushch, L. V. Zorina, S. S. Khasanov, R. P. Shibaeva, T. G. Togonidze, A. E. Kovalev, M. V. Kartsovnik, L. I. Buravov, E. B. Yagubskii, E. Canadell, A. Kobayashi, and H. Kobayashi, Eur. Phys. J. B **5**, 179 (1998).
- ³⁴ H. Kobayashi, R. Kato, A. Kobayashi, Y. Nishio, K. Kajita, and W. Sasaki, Chem. Lett. 883, (1986).
- ³⁵ T. Mori, Bull. Chem. Soc. Jpn., **71**, 2509 (1998).
- ³⁶ D. Beckmann, S. Wanks, J. Wosnitzer, D. Schweitzer and W. Strunz, Z. Phys. B **104**, 207 (1997).
- ³⁷ Y. N. Xu, W. Y. Ching, Y. C. Jean and Y. Lou, Phys. Rev. B **52** 12946 (1995).
- ³⁸ R. C. Haddon, A. P. Ramirez, and S. H. Glarum, Adv. Mater. **6**, 316 (1994).
- ³⁹ W. Y. Ching, Y. N. Xu, Y. C. Jean, and Y. Lou, Phys. Rev. B **55** 2780 (1997).

- ⁴⁰ B. Andraka, J. S. Kim, G. R. Stewart, K. D. Carlson, H. H. Wang and J. M. Williams, Phys. Rev. B **40** 11345 (1989).
- ⁴¹ C. H. Mielke, N. Harrison, D. G. Rickel, A. H. Lacerda, R. M. Vestal, and L. K. Montgomery, Phys. Rev. B **56**, R4309 (1997).
- ⁴² B. Andraka *et al*, Solid State Commun. **79**, 57 (1991).
- ⁴³ H. Elsinger, J. Wosnitza, S. Wanka, J. Hagel, D. Schweitzer, and W. Strunz, cond-mat/9912031.
- ⁴⁴ J. Wosnitza, X. Liu, D. Schweitzer, and H. J. Keller, Phys. Rev. B **50**, 12747 (1996).
- ⁴⁵ G. R. Stewart, J. O'Rourke, G. W. Crabtree, K. D. Carlson, H. H. Wang, J. M. Williams, F. Gross, and K. Andres, Phys. Rev. B **33**, 2046 (1986).